Preprint DFPD 02/TH/04 (Univ. of Padua) 1–26 (2008)

Three-Body Dynamics in One Dimension: A Test Model for the 3-Nucleon System with Irreducible Pionic Diagrams

T. Melde [1], L. Canton[1,2], J.P. Svenne [3]

[1] Dipartimento di Fisica, Università di Padova, Via F. Marzolo 8, Padova, Italy, I-35131
[2] Istituto Nazionale di Fisica Nucleare, Sezione di Padova, Via F. Marzolo 8, Padova, Italy, I-35131
[3] Winnipeg Institute for Theoretical Physics and Department of Physics and Astronomy, University of Manitoba, Winnipeg, MB, Canada R3T 2N2

Abstract. We formulate the three-body problem in one dimension in terms of the (Faddeev-type) integral equation approach. As an application, we develop a spinless, one-dimensional (1-D) model that mimics three-nucleon dynamics in one dimension. Using simple two-body potentials that reproduce the deuteron binding, we obtain that the three-body system binds at about 7.5 MeV. We then consider two types of residual pionic corrections in the dynamical equation; one related to the 2π-exchange three-body diagram, the other to the 1π-exchange three-body diagram. We find that the first contribution can produce an additional binding effect of about 0.9 MeV. The second term produces smaller binding effects, which are, however, dependent on the uncertainty in the off-shell extrapolation of the two-body t-matrix. This presents interesting analogies with what occurs in three dimensions. The paper also discusses the general three-particle quantum scattering problem, for motion restricted to the full line.

1 Introduction

The quantum mechanics of one-dimensional systems has always attracted interest in various research fields and has been extensively studied and investigated for a variety of purposes, ranging from the study of exactly solvable many-body systems [1], to the phenomenological description of tunneling phenomena [2] in quantum wires, semiconductors, or across junctions [3]. The mathematical properties for the underlying Schrödinger operators have been recently reviewed in ref. [4]. Quantum scattering in one dimension has been also considered because of its value in pedagogical works [5, 6, 7], since it retains sufficient complexity to embody many of the physical concepts and behaviours that occur in the more

complex three-dimensional processes, but without the many technical aspects required for dealing with quantum scattering in higher dimensions.

One-dimensional models are furthermore often constructed to gain deeper insight into the methods and approximations introduced to reduce the complexity of the higher-dimensional cases. In this spirit, we developed a one dimensional three-body model with the scope of testing three-nucleon theories in a simplified environment. We are in particular interested in the formulation of the quantum three-body theory on the full, $(-\infty, +\infty)$ line, based on a system of coupled integral equations for the three-body transition operators (AGS equations [8], extended to an arbitrary number of bodies by Grassberger and Sandhas [9]). The approach is directly linked to the first mathematical theory of three-body scattering by Faddeev [10], based on the integral formulation for the three-body Green's function and extended to N bodies by Yakubovski [11].

The formulation of the one-dimensional three-body problem in terms of the Faddeev-AGS scattering theory represents a somewhat "unusual" problem, since one-dimensional scattering corresponds also to the potential-barrier problem, which therefore has to be implemented with the clustering structure of the three-body problem. We illustrate in this paper an approach that harmonizes the typical two-channel structure of the "tunneling" problems, due to the presence of the transmission and reflection processes, with the cluster structure of the three-body problem, thus leading to an overall reduced S-matrix for the two-fragment processes which is 6×6. The formulation presented herein, with straightforward modifications, is suited also to describe the tunneling (or potential-barrier) effects due to the scattering of a two-body one-dimensional cluster impinging on an external barrier potential. A 3-D application along this line already has been discussed for a molecular system [12].

The present work was motivated by the need to develop a simplified, 1-D test model for the non-relativistic treatment of the system consisting of three nucleons interacting via exchanges of a force-mediating "pion" (plus some shorter-range contributions). In modern three-nucleon dynamics, one of the crucial problems involves the treatment of those additional mesonic contributions that cannot be effectively described by the standard nucleon-nucleon potentials. Such terms are generally referred to as irreducible three-nucleon-force (3NF) contributions and are used to construct a phenomenological 3N potential. The hope is to cure in this way the discrepancies observed between experiments and rigorous Faddeev three-body calculations with realistic 2N potentials [13, 14]. The subsequent employment of the newer high-precision 2N potentials [15, 16, 17] essentially confirmed the existence of such discrepancies. For example, the three-nucleon bound state, the triton, is typically under-bound by the high-precision NN potentials and the vector analyzing powers are substantially underestimated for low-energy nucleon-deuteron scattering (the so-called A_y-puzzle) [18, 19].

Considerable progress has been made since the introduction of 3NF based on isobars by Fujita and Miyazawa [20], leading to a number of different 3NFs [21, 22, 23, 24] in use today, that can all be adjusted to describe adequately the triton binding energy. However, none of these terms have solved also the A_y-puzzle, which suggests that work still needs to be done to understand the role of

the 3NF terms in few-nucleon systems. A few years ago, an approach has been developed [25] that reduces the field theoretic problem of the pion-three-nucleon dynamics to an approximate set of integral equations for the coupled πNNN-NNN system. The method extends the standard AGS formulation to the case of a three-body system with the additional pionic degree of freedom. The resulting equations merge together the Faddeev structure for the three-nucleon sector with the Yakubovski structure of the four-body sector, and has been shown to possess a kernel which is connected after iterations.

Recently [26], a practical approximation scheme for the treatment of this coupled πNNN-NNN system has been proposed. The scheme is based on the assumption that the dominant part of the pion-exchange processes can be effectively described by contributions to the 2N potential, while the residual mesonic aspects lead to the addition of smaller, correction-type, 3NF effects. This assumption forms the basis for the standard description of nuclear systems in terms of aggregates of (pairwise) interacting nucleons, and ultimately relies on the chiral nature of the hadron interactions [24]. The irreducible 3NF corrections due to the residual pion dynamics are treated perturbatively in the extended AGS equation, which is further reduced to an effective two-body integral equation in the inter-cluster momentum variable, by means of a finite-rank expansion of the two-nucleon potential.

At the lowest order, the residual pion dynamics produced irreducible correction contributions to the driving term of the AGS equation, and one type of these corrections can be identified with the so-called 2π-exchange 3NF diagram, and leads to the force models discussed, e.g., in refs. [20, 21, 22, 23, 24]. But at the same time, the approach produced also another type of irreducible pionic diagrams [26, 27] – the 1π-exchange 3NF term – that could not be identified with any previously known 3NF expression and which, as shown in completely realistic situations [28, 29], has the potential to solve the A_y problem. For a brief review, see also ref. [30].

In the following, we develop a one-dimensional spinless model that mimics three-nucleon dynamics in one dimension. In particular, we investigate numerically the effects of these irreducible "pionic" corrections in the one-dimensional three-body bound state by solving the homogeneous version of the AGS equation. This 1-D model was originally constructed as a laboratory to investigate the dynamical effects of the meson on the three-body bound state [31]. However, one-dimensional systems in themselves are of considerable interest [32, 33, 34] and in many ways different from the three-dimensional case. This difference manifests itself, for example, in the existence of only two partial waves [7, 35, 36] and the different structure of Levinson's theorem [37, 38, 39].

Section 2 presents the AGS form of the three-body theory on the line, and its reduction to a Lovelace-type equation for a symmetrized three-particle system interacting via separable potentials. In Sect. 3 we define the explicit form of the pionic correction terms to the Lovelace-AGS equation. In Sect. 4 we consider the homogeneous version of the three-body integral equation, which leads to the calculation of the binding energies. In Sect. 5 we discuss the details of the three-body model and illustrate the results obtained. For the conclusions and a

summary of the results we refer to Sect. 6.

Finally, we have also endowed this work with three appendices, devoted to specific aspects of the one-dimensional two-body system. Appendix A illustrates the integral formulation of the one-dimensional two-body scattering problem. Although the treatment can be found in the literature, e.g. in ref. [7], the discussion presented in the Appendix stresses the analogies with the three-body problem. Also the low-energy expansion of the two-body amplitudes is discussed therein. Appendix B illustrates the details for the expansion of the 2-body potentials in a finite-rank form, along the lines of the Unitary Pole Expansion (UPE) method. Appendix C discusses the method we have employed to solve numerically the one-dimensional two-body problem in one dimension, for both bound-state and scattering regimes.

2 The Alt-Grassberger-Sandhas Three-Body Theory on the Full Line

2.1 Distinguishable Particles

In this section we formulate the Faddeev-AGS theory for three distinguishable particles moving in one dimension, $(-\infty, +\infty)$. We consider three spinless particles interacting only with 2-body potentials, and assume that these potentials are short-range, or at most exponentially decaying when the inter-particle distance goes to infinity. The case of irreducible 3NF-type diagrams will be discussed in Sect. 3. For simplicity, the two-body potential is assumed to support only one bound-state, as happens for the 2-nucleon system, but the formulation can be easily generalized to the case of a finite number of bound states. The particles are labeled "1", "2", and "3", and the indices $a, b, c, \ldots$ range over the three labels. We will adhere to the odd-man-out notation which implies that when $a = 1$, for example, V_a denotes the interaction between the pair (23).

A system of three particles is described by the Hamiltonian

$$H = H_0 + \sum_a V_a \,. \tag{1}$$

We then introduce the channel states, which are eigenstates of the channel Hamiltonians

$$H_a = H_0 + V_a \,, \tag{2}$$

with $a = 1, 2, 3$. The full Hamiltonian can also be written as

$$H = H_a + V^a \,, \tag{3}$$

where

$$V^a = \sum_{b \neq a} V_b \tag{4}$$

denotes the interaction "external" to channel a. In the one-dimensional system the channel states can be described by the following wave functions

$$\Phi_{\pm a} = \Phi_{\pm q_a}\left(x_a, y_a\right) = e^{\pm \mathrm{i} q_a y_a} \phi_a\left(x_a\right) \,, \tag{5}$$

where $\phi_a(x_a)$ denotes the properly normalized bound-state wave function of the two-particle fragment and $e^{\pm \mathrm{i} q_a y_a}$ denotes the relative motion of the particle a with respect to the c.m. of the two-particle fragment (bc). Here, x_a, y_a are the Jacobi coordinates for partition $a\,(bc)$ and q_a is the relative momentum between particle a and the cluster (bc). The $\pm$ in the channel wave function is due to the presence of two physically different states, one with an incoming wave from the left and one with an incoming wave from the right. Note that this definition implicitly assumes $q_a \geq 0$. Alternatively, we define also

$$\Phi_a = \Phi_{q_a}(x_a, y_a) = e^{\mathrm{i} q_a y_a} \phi_a(x_a) \,, \tag{6}$$

where q_a may assume also negative values.

The channel wave functions are eigenstates of the channel Hamiltonian H_a with the eigenvalue

$$E_a = \frac{\hbar^2 {q_a}^2}{2M_a} + \hat{E}_a \,, \tag{7}$$

where $\hat{E}_a$ is the bound state energy of the two-particle fragment and M_a is the reduced mass of particle a and the cluster (bc). The masses of the three (identical) particles are given by $m_N c^2 = 938.27$ MeV, the mass of the pion is $m_\pi c^2 = 134.98$ MeV and the reduced mass of the particles b, c is μ_a. Furthermore, because we consider three identical particles we also have $\mu_a = \mu_b = \mu_c = \mu$ and $M_a = M_b = M_c = M$.

Let us assume an asymptotic 1-D plane wave incoming from the left, described by the channel wave functions Φ_{+a}. Then we can have three different transmitted two-cluster waves, and similarly for the reflected terms, which leads to the asymptotic form

$$\Psi_a^L(x, y) \to \begin{cases} \Phi_{+b}\delta_{ab} + R_{ab}^L(E)\,\Phi_{-b}, & \text{for } y_b \to -\infty \\ T_{ab}^L(E)\,\Phi_{+b}, & \text{for } y_b \to +\infty \end{cases} \tag{8}$$

where x, y is a generic set of Jacobi coordinates. The superscript L reflects the fact that the incident wave is coming from the left. Differently from the two-body case where there is only one single channel, we are now in a multichannel situation where the rearrangement processes (i.e., $a \neq b$) have to be also described. This leads to the definition of the reduced S-matrix for two-fragment scattering which is formally equivalent to the one defined in Appendix A for two-particle scattering, but features in addition the cluster labels,

$$\tilde{\mathbf{S}}_{\mathbf{ab}}(E) = \begin{pmatrix} T_{ab}^L(E) & R_{ab}^R(E) \\ R_{ab}^L(E) & T_{ab}^R(E) \end{pmatrix} . \tag{9}$$

This definition produces a 6×6 scattering matrix connecting all six possible "two-fragment asymptotic channels" $\Phi_{\pm a}$. The occurrence of such type of S-matrix has been observed already in the framework of an exactly soluble problem in ref. [40]

To solve the one-dimensional three-body scattering problem the S-matrix has to be determined, and for this we use the known expression [41]

$$\langle \Phi_a | S_{ab} | \Phi_b \rangle = \delta_{ab}\delta(q_a - q_b) - 2\pi i \delta(E_a - E_b) \langle \phi_a | V^a | \Psi_b \rangle \,. \tag{10}$$

It is then possible to introduce [42] the transition operators U_{ab}, with the definition

$$\langle \Phi_a | \, U_{ab} \, | \Phi_b \rangle = \langle \Phi_a | \, V^a \, | \Psi_b \rangle \ , \tag{11}$$

which satisfy the operatorial Alt-Grassberger-Sandhas equation

$$U_{ab} = \bar{\delta}_{ab} G_0^{-1} + \sum_c \bar{\delta}_{ac} V_c G_c U_{cb} \ , \tag{12}$$

where $\bar{\delta}_{ab} = 1 - \delta_{ab}$ and $G_a(z) = (z - H_a)^{-1}$. To recover the 6×6 structure for the reduced S-matrix we decompose the momentum on the line

$$q = |q| \, \mathrm{sign}(q) \ , \tag{13}$$

where $\mathrm{sign}(q)$ denotes the sign of q. Then, we consider the two delta functions in the expression of the S-matrix, Eq. (10),

$$\delta(q_a - q_b) = \delta(|q_a| - |q_b|) \, \delta_{\mathrm{sign}(q_a)\,\mathrm{sign}(q_b)} \ , \tag{14}$$

and

$$\delta(E_a - E_b) = \frac{2M}{\hbar^2} \delta\left(|q_a|^2 - |q_b|^2 \right) = \frac{M}{\hbar^2 |q_b|} \delta(|q_a| - |q_b|) \ . \tag{15}$$

In this last equation we have assumed for simplicity that the bound-state energies of any two-particle fragments are the same. The generalization to the case with different binding energies, i.e. $\hat{E}_a \neq \hat{E}_b$ for $a \neq b$, is straightforward. Therefore, the S-matrix can be written as

$$\langle \Phi_a | \, S_{ab} \, | \Phi_b \rangle = \delta(|q_a| - |q_b|) \, \langle \Phi_{\pm a} | \, \tilde{S}_{ab} \, | \Phi_{\pm b} \rangle \ , \tag{16}$$

where

$$\begin{aligned} &\tilde{\mathbf{S}}_{\mathbf{ab}}(E) = \langle \phi_{\pm a} | \, \tilde{S}_{ab} \, | \phi_{\pm b} \rangle \\ &= \delta_{ab} \begin{pmatrix} 1 & 0 \\ 0 & 1 \end{pmatrix} - 2\pi \frac{\mathrm{i}M}{\hbar^2 |q_b|} \begin{pmatrix} t_{ab}(+|q_a|, +|q_b|; E) & t_{ab}(+|q_a|, -|q_b|; E) \\ t_{ab}(-|q_a|, +|q_b|; E) & t_{ab}(-|q_a|, -|q_b|; E) \end{pmatrix} . \end{aligned} \tag{17}$$

To solve the AGS equation we expand the 2-body potentials into a finite-rank form. The method of expansion is discussed in Appendix B. For simplicity, in this section we illustrate the formulation for the case of a separable (rank-one) expression for the 2-body potentials

$$V_a^{sep} = \frac{V_a |\phi_a\rangle \langle \phi_a | V_a}{\langle \phi_a | V_a | \phi_a \rangle} \, , \tag{18}$$

where $|\phi_a\rangle$ corresponds to the properly normalized bound-state of the two-body subsystem a. Then the AGS equation transforms into an effective two-cluster Lovelace-type equation for the transition amplitudes [43], which is an integral equation in the inter-cluster momentum variable,

$$\begin{aligned} X_{ab}(q_a, q_b; E) &= Z_{ab}(q_a, q_b; E) \\ &\quad + \sum_c \int_{-\infty}^{+\infty} Z_{ac}(q_a, q_c; E) \, \Delta_c(q_c; E) \, X_{cb}(q_c, q_b; E) \, dq_c \, . \end{aligned} \tag{19}$$

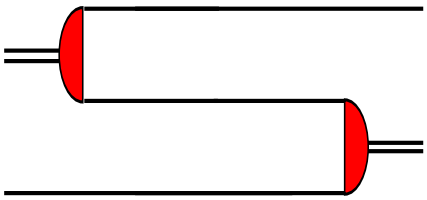

Figure 1. The exchange diagram, representing the AGS driving term

The driving term of this equation corresponds to the exchange diagram represented in Fig. 1, and is calculated according to the expression [44]

$$Z_{ab}\left(q_a, q_b, E\right) = \frac{\chi_a\left(\frac{q_a}{2} + q_b\right)\chi_b\left(-q_a - \frac{q_b}{2}\right)}{E - \frac{\hbar^2}{2m_N}\left(q_a^2 + \left(q_a + q_b\right)^2 + \left(q_b\right)^2\right)}\,. \tag{20}$$

Note that there is also a second driving term Z_{ac} with $a \neq c \neq b \neq a$ and implying the appropriate Jacobi-coordinate transformations. The $\Delta_a\left(q_a; E\right)$ is given by

$$\Delta_a\left(q_a; E\right) = \left[\int_{-\infty}^{+\infty} \phi_a(p)\chi_a(p)dp - \int_{-\infty}^{+\infty} \frac{\chi_a(p)\chi_a(p)dp}{E - \frac{(\hbar q_a)^2}{2M} - \frac{(\hbar p)^2}{2\mu}}\right]^{-1}\,. \tag{21}$$

In these last equations we have also introduced the form factors of the separable interaction, $|\chi_a\rangle = V_a|\phi_a\rangle$, for convenience.

Once evaluated for the on-shell momenta, the solution of this integral equation provides the transition amplitudes

$$\langle\phi_{\pm a}|\, U_{ab}\, |\phi_{\pm b}\rangle = X_{ab}\left(\pm|q_a|, \pm|q_b|; E\right) = t_{ab}(\pm|q_a|, \pm|q_b|; E)\,, \tag{22}$$

which are needed in Eq. (17) for the construction of the S-matrix.

2.2 Symmetrization

Lovelace [43] has discussed how the system of coupled equations can be symmetrized, leading to a single-channel integral equation

$$\mathcal{X}\left(q, q'; E\right) = \mathcal{Z}\left(q, q'; E\right) + \int_{-\infty}^{+\infty} \mathcal{Z}\left(q, q''; E\right)\Delta\left(q''; E\right)\mathcal{X}\left(q'', q'; E\right)dq''\,. \tag{23}$$

The q, q', and q'' denote the inter-cluster momentum variables of the two-fragment states. The function $\Delta\left(q''; E\right)$ is the same as calculated in Eq. (21), while the symmetrized driving term $\mathcal{Z}\left(q, q''; E\right)$ is now twice that calculated in Eq. (20). The method works for both bosons and fermions, the difference between the two being in the representation of the two-body sub-amplitude. For bosons, the two-body t-matrix has to be expanded via the UPE method using only symmetric states, i.e., with the even functions $\chi_i(p) = \chi_i(-p)$. In the case of three identical particles only one type of two-cluster partition is observable,

and therefore the 6×6 structure of the previously defined S-matrix and of the transition amplitude collapses back into a 2×2 structure, as was for the case of two-body scattering.

The $\mathcal{X}(q, q'; E)$ represent the two-fragment transition amplitude which has to be evaluated, for a given energy E, at the only two possible on-shell values for q, q'. These momenta have to satisfy the condition

$$q^2 = {q'}^2 = \frac{2M}{\hbar^2}(E - E_D) = \frac{2M}{\hbar^2}\bar{E}\,, \tag{24}$$

where E_D is the bound state energy of the two-particle fragment. Because the system is defined on the real line, the values for the inter-cluster momenta have to be

$$|q| = \sqrt{\frac{2M}{\hbar^2}(E - E_D)} = \sqrt{\frac{2M\bar{E}}{\hbar^2}}\,. \tag{25}$$

This allows us to write the S-matrix for one-dimensional $2+1$ scattering in the following way

$$S(E) = \begin{pmatrix} 1 & 0 \\ 0 & 1 \end{pmatrix} - 2\pi \frac{\mathrm{i}M}{\hbar^2 |q|} \begin{pmatrix} \mathcal{X}(|q|, |q|; E) & \mathcal{X}(|q|, -|q|; E) \\ \mathcal{X}(-|q|, |q|; E) & \mathcal{X}(-|q|, -|q|; E) \end{pmatrix}, \tag{26}$$

which has the same structure as the two-body S-matrix defined in Appendix A.

3 Treatment of the Irreducible Pionic Corrections

The method, discussed up to now for a separable (i.e., rank one) expression for the two-body interaction, has to be extended to a rank-N expansion, as described in Appendix B. The symmetrized Lovelace-type equation for a rank-N potential is given by

$$\begin{aligned} \mathcal{X}_{ij}(q, q'; E) = {} & \mathcal{Z}_{ij}(q, q'; E) \\ & + \sum_{k,l}^{N} \int_{-\infty}^{+\infty} \mathcal{Z}_{ik}(q, q''; E)\, \Delta_{kl}(q''; E)\, \mathcal{X}_{lj}(q'', q'; E)\, dq''\,, \end{aligned} \tag{27}$$

where Δ_{kl} is defined in Appendix B. The driving terms acquire a matrix structure in the rank space, $\mathcal{Z}_{ij}$.

Typically, the symmetrized Lovelace equation leads to a driving term

$$\mathcal{Z}_{ij} = 2Z_{ij}^{N}\,, \tag{28}$$

which is twice that calculated in Eq. (20). The label "N" in the above expression is a reminder of the off-diagonal character of the driving term, due to the presence of $\bar{\delta}_{ab}$ in Eq. (12). The factor 2 arises because in the symmetrized Lovelace three-body equation there are two off-diagonal elements that add coherently.

The three-body Lovelace-type integral equation can be extended to include the degrees of freedom of one single meson [25]. To reduce the complexity of the resulting equation, one can consider a simplified formulation [26] where the effects

of the two-body interactions are treated exactly, and the residual irreducible (3NF-like) mesonic effects are treated approximately, as "first-order" corrections. The approximation scheme leads to mesonic corrections to the driving term, Eq. (20), of the standard three-body equation with two-body potentials discussed in the previous section.

These pionic corrections corrections modify the driving term according to the expression

$$\mathcal{Z}_{ij} = Z_{ij}^{D} + 2Z_{ij}^{N}\,, \tag{29}$$

where the superscript D denotes now the presence of diagonal-type contributions. Without these corrections one recovers the standard AGS-term by considering only the off-diagonal elements [44], i.e., $Z_{ij}^{D} = 0$, and $Z_{ij}^{N} = Z_{ij}^{AGS}$.

In particular, the standard AGS term in the N-rank case is given by

$$Z_{ij}^{AGS}\left(q,q',E\right) = \frac{\chi_i\left(\frac{q}{2}+q'\right)\chi_j\left(-q-\frac{q'}{2}\right)}{E-\frac{\hbar^2}{2m_N}\left(q^2+\left(q+q'\right)^2+\left(q'\right)^2\right)}\,, \tag{30}$$

where the form factors χ_i, χ_j are defined in Appendix B. We remind also that, since we have assumed a bosonic structure of the particles, only the even parity form factors are included in the separable expansion.
The treatment of the irreducible pionic effects leads one to consider, in first approximation, the following correction terms

$$Z_{ij}^{N} = Z_{ij}^{AGS} + Z_{ij}^{TPE3} \tag{31}$$

$$Z_{ij}^{D} = Z_{ij}^{OPE3}\,. \tag{32}$$

The diagrams generating these two additional terms are reported in Figs. 2 and 3, for Z^{TPE3} and Z^{OPE3}, respectively (we recall that the standard AGS exchange diagram was reported in Fig. 1).

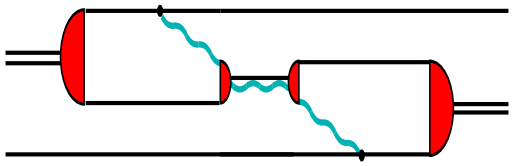

Figure 2. Correction terms to the off-diagonal AGS driving term

The off-diagonal correction terms are given by

$$Z_{ij}^{TPE3}\left(q,q',E\right) = \int \frac{\chi_i\left(p\right)}{E-\frac{\left(\hbar q\right)^2}{2M}-\frac{\left(\hbar p\right)^2}{2\mu}} V^{TPE3}\left(p,p',q,q'\right) \frac{\chi_j\left(p'\right)}{E-\frac{\left(\hbar q'\right)^2}{2M}-\frac{\left(\hbar p'\right)^2}{2\mu}} dpdp'\,, \tag{33}$$

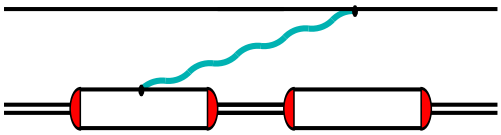

Figure 3. Correction terms to the diagonal AGS driving term.

and similarly for the diagonal correction terms,

$$Z_{ij}^{OPE3}\left(q,q',E\right) = \int \frac{\chi_i\left(p\right)}{E-\frac{(\hbar q)^2}{2M}-\frac{(\hbar p)^2}{2\mu}} V^{OPE3}\left(p,p',q,q'\right) \frac{\chi_j\left(p'\right)}{E-\frac{(\hbar q')^2}{2M}-\frac{(\hbar p')^2}{2\mu}} dpdp' \,. \quad (34)$$

The first contribution to the driving term $\mathcal{Z}_{ij}$ is generated by an intermediate πN re-scattering process, as depicted by the diagram in Fig. 2. In the static approximation, the amplitude for such a process is given by the expression

$$V^{TPE3}\left(p,p',q,q'\right) = \frac{f^2}{\pi} \frac{\hat{t}_{\pi N}}{\left(Q^2+\left(\frac{m_\pi c}{\hbar}\right)^2\right)\left(\left(Q'\right)^2+\left(\frac{m_\pi c}{\hbar}\right)^2\right)} \,. \quad (35)$$

Here, the Q, Q' are the pion momenta in the center of mass system with the proper set of Jacobi momenta

$$Q = p - \frac{q}{2} - q' \quad (36)$$

$$Q' = -q - p' - \frac{q'}{2} \quad (37)$$

and $\hat{t}_{\pi N}$ denotes the πN amplitude.

One serious difficulty inherent to this test model was connected with the construction of this one-dimensional πN amplitude, since this represents a completely abstract entity, which has no direct link to the phenomenological, three-dimensional amplitude of the real world [1]. We decided to circumvent this difficulty by observing that the πN scattering lengths are roughly between one and two orders of magnitude smaller than the corresponding 2N scattering lengths [45]. This suggests that probably the most simple parametrization for the πN amplitude in one dimension is to take the low-energy limit of the corresponding 2N one-dimensional amplitude, and to divide this amplitude by a factor c_1 between 10 and 100. The low-energy expansion for the two-body t-matrix is

[1] It should be noted that, in obtaining the 3NFs in the full three-dimensional form, this πN scattering amplitude is also the main source of uncertainty due to the need to find a satisfactory off-shell extension and suitable pion form factors [22].

discussed in Appendix A, to which we refer for the details. The result leads to the following low-energy structure for the 1-D πN amplitude

$$\hat{t}_{\pi N}\left(Q,Q'\right) \approx -\frac{1}{c_1}\left[\left(\hat{\alpha}_0+\hat{\alpha}_1\right)|Q|\left|Q'\right|+\left(\hat{\alpha}_0-\hat{\alpha}_1\right)QQ'\right] , \tag{38}$$

where the parameter c_1 has been arbitrarily set to $c_1=-15$, to be approximately consistent with the ratio between the observed scattering lengths of the πN and NN systems.

Therefore, the final result for this contribution has the following structure

$$\begin{aligned} Z_{ij}^{TPE3}\left(q,q',E\right) &= -\frac{f^2}{c_1\pi}\left(\hat{\alpha}_0+\hat{\alpha}_1\right)\int\frac{|Q|}{Q^2+\left(\frac{m_\pi c}{\hbar}\right)^2}\frac{\chi_i\left(p\right)}{E-\frac{\left(\hbar q\right)^2}{2M}-\frac{\left(\hbar p\right)^2}{2\mu}}dp \\ &\times\int\frac{|Q'|}{\left(Q'\right)^2+\left(\frac{m_\pi c}{\hbar}\right)^2}\frac{\chi_j\left(p'\right)}{E-\frac{\left(\hbar q'\right)^2}{2M}-\frac{\left(\hbar p'\right)^2}{2\mu}}dp' \\ &-\frac{f^2}{c_1\pi}\left(\hat{\alpha}_0-\hat{\alpha}_1\right)\int\frac{Q}{Q^2+\left(\frac{m_\pi c}{\hbar}\right)^2}\frac{\chi_i\left(p\right)}{E-\frac{\left(\hbar q\right)^2}{2M}-\frac{\left(\hbar p\right)^2}{2\mu}}dp \\ &\int\frac{Q'}{\left(Q'\right)^2+\left(\frac{m_\pi c}{\hbar}\right)^2}\frac{\chi_j\left(p'\right)}{E-\frac{\left(\hbar q'\right)^2}{2M}-\frac{\left(\hbar p'\right)^2}{2\mu}}dp' . \end{aligned} \tag{39}$$

We stress that the arguments to arrive at the form Eq. (38) for the subtracted πN amplitude have been ultimately quite arbitrary; however they reproduce the net result that, in the limit $c_1\to\infty$, that is when the πN scattering length is much smaller than the 2N scattering length, the corresponding 3NF effect vanishes. The second contribution, V^{OPE3}, is generated by the diagram in Fig. 3. The corresponding amplitude is obtained by summing over four terms, namely [27]

$$\begin{aligned} V^{OPE3}\left(p,p',q,q'\right) &= f_1G_0^{(4)}\tilde{t}_{12}G_0^{(4)}f_3^\dagger+f_2G_0^{(4)}\tilde{t}_{12}G_0^{(4)}f_3^\dagger \\ &+f_3G_0^{(4)}\tilde{t}_{12}G_0^{(4)}f_1^\dagger+f_3G_0^{(4)}\tilde{t}_{12}G_0^{(4)}f_2^\dagger , \end{aligned} \tag{40}$$

where $G_0^{(4)}$ is the 4-particle free propagator and f_i denotes the creation operator of a pion on nucleon i, while $f_i^\dagger$ denotes the destruction of a pion on nucleon i. The quantity $\tilde{t}_{12}$ describes the two-body t-matrix for nucleons $1,2$. Similarly to the case of the TPE3-term, also in this case one has to include a cancellation effect, since one must subtract from the two-body amplitude the corresponding "Born terms", i.e. the meson-exchange contributions, which can be identified with the two-body potential itself. Furthermore, the two-body t-matrix entering in this diagram has to be evaluated in a region which is substantially off-shell, because of the role of the exchanged meson in this diagram. Therefore, following the studies of refs. [27, 28, 29] we have considered the effective parameter that governs the cancellation for the diagonal correction terms:

$$\tilde{t}_{12}\left(p,p';z\right)=c_2t_{12}\left(p,p';z\right)-v_{12}\left(p,p'\right) , \tag{41}$$

where

$$z=E-\frac{\left(\hbar q\right)^2}{2M}-\hbar c\omega_\pi\left(Q\right) . \tag{42}$$

The effective parameter c_2 represents an overall correction factor for the far-off-the-energy-shell extrapolation of the t-matrix [28, 29]. Also, v_{12} denotes the meson exchange contributions as defined in the nucleon-nucleon potential acting between nucleons $1, 2$ and

$$\omega_\pi(Q) = \sqrt{Q^2 + \frac{m_\pi^2 c^2}{\hbar^2}} \tag{43}$$

is the relativistic pion energy with the pion momentum

$$Q = q - q' . \tag{44}$$

Using a static approximation for the four-body Green's functions $G_0^{(4)}$ and inserting the explicit expressions for the creation and destruction operators gives the following form for the static contribution to the diagonal correction terms

$$V^{OPE3}(p,p',q,q') = \frac{f^2}{\pi}\frac{2}{\hbar c\omega_\pi^3(Q)} \times \left[\tilde{t}_{12}\left(p,p';E-\frac{(\hbar q)^2}{2M}-\hbar c\omega_\pi(Q)\right)+\tilde{t}_{12}\left(p,p';E-\frac{(\hbar q')^2}{2M}-\hbar c\omega_\pi(Q)\right)\right] . \tag{45}$$

In this paper we are using the unitary-pole expansion and consequently the subtracted NN t-matrix is defined as

$$\tilde{t}_{12}\left(p,p';E-\frac{(\hbar q)^2}{2M}-\hbar c\omega_\pi(Q)\right) = \sum_{ij}\chi_i(p)\left(c_2\Delta_{ij}\left(E-\frac{(\hbar q)^2}{2M}-\hbar c\omega_\pi(Q)\right)+\eta_i^{-1}\delta_{ij}\right)\chi_j(p') , \tag{46}$$

which leads to the final expression for the diagonal contribution of the correction term in a rank-N separable expansion

$$Z_{ij}^{OPE3}(q,q',E) = \frac{f^2}{\pi}\frac{2}{\hbar c\omega_\pi^3(Q)}\left\{\sum_{kl}\int\frac{\chi_i(p)\chi_k(p)}{E-\frac{(\hbar q)^2}{2M}-\frac{(\hbar p)^2}{2\mu}}dp \times\left[c_2\Delta_{kl}\left(E-\frac{(\hbar q)^2}{2M}-\hbar c\omega_\pi(Q)\right)+c_2\Delta_{kl}\left(E-\frac{(\hbar q')^2}{2M}-\hbar c\omega_\pi(Q)\right)+2\eta_k^{-1}\delta_{kl}\right] \times\int\frac{\chi_l(p')\chi_j(p')}{E-\frac{(\hbar q')^2}{2M}-\frac{(\hbar p')^2}{2\mu}}dp'\right\} . \tag{47}$$

This fully defines the driving term of the rank-N symmetrized Lovelace-type equation.

4 Bound-state equation

In the previous sections we have provided the AGS formulation for three-body scattering in one dimension. However, we will now restrict the discussion to the corresponding bound-state problem. We will apply this formalism to the calculation of the binding energies, as a first test for analyzing the effects of the irreducible pionic corrections in the 1-D three-body system. As is known, the Faddeev or AGS method formulates the scattering problem in terms of an inhomogeneous integral equation which can be reduced, after iteration, to one of Fredholm type. Such equations are known [46] to have no solution in case the related homogeneous equation admits non-trivial solutions, which are associated with bound states.

A further step, introduced for the convenience of numerical solution of the homogeneous AGS-Lovelace Eq. (27), is to express it in the form of a sturmian eigenvalue problem [47]. Therefore, in order to find the three-body bound state energy, we solve the generalized eigenvalue equation [48]

$$\sum_j \int \mathcal{U}_{ij}\left(q,q',E\right)\psi_{jk}\left(q'\right)dq' = \eta_k\left(E\right)\sum_j \int \mathcal{Z}_{ij}\left(q,q',E\right)\psi_{jk}\left(q'\right)dq' \,. \quad (48)$$

In this equation

$$\mathcal{U}_{ij}\left(q,q',E\right) = \sum_{kl}\int \mathcal{Z}_{ik}\left(q,q'',E\right)\Delta_{kl}\left(q'';E\right)\mathcal{Z}_{lj}\left(q'',q',E\right)dq'' \,, \quad (49)$$

and the remaining quantities are the same as those defined in Sect. 3. The eigenvalues $\eta_k\left(E\right)$ are energy-dependent, because of the dependence on the energy of $\mathcal{Z}$ and Δ. The energy is varied, and the bound-state energies of the three-body system are found by the condition that the eigenvalue be equal to one at $E = E_B$. Since the binding energy is negative, all integrals (in Sect. 3) involving the Green's function are nonsingular, while for energies above the scattering threshold, whenever such integrals become singular, they have to be regularized with suitable subtraction techniques.

5 Results of the Test Model

We have constructed three different two-body potentials that mimic the nuclear force on the line. The general structure of these potentials is given by

$$V\left(x\right) = V_A e^{-\beta|x|} + V_R e^{-n\beta|x|} \,, \quad (50)$$

with the free parameters V_A, V_R. In Table 1 we report the three different sets of parameters. The range parameter β of the attractive part is the inverse of the Compton wavelength of the pion

$$\beta = \frac{m_\pi c}{\hbar} \,, \quad (51)$$

which we consider fixed. The range parameter of the repulsive part is variable and has been parametrized in terms of multiples of β, denoted as n. That is, n denotes

the ratio between the Compton wavelength of the "scalar pion", the boson that mediates the attraction component, and that of the repulsive short-range component. For the purpose of the upcoming discussion it is unimportant whether the short-range part is mediated by heavy-boson exchange, or by a generic cut-off mechanism which suppresses the contributions coming from momenta higher than the cut-off parameter. Three values for n have been selected, 5, 10, and 20, corresponding to an increasing "stiffness" of the short-range repulsion.

The remaining parameters were fitted to reproduce a two-body bound state at (approximately) the deuteron energy and a two-body low-energy scattering parameter at about 24 fm, which would then correspond to the 1-D equivalent of the NN scattering length. The binding energies reported in Table 1 were

Table 1. Strength and range parameters of the one dimensional potentials approximating nuclear physics and the imaginary parts of the low energy expansion parameters

	n	V_A [MeV]	V_R [MeV]	$\hat{\alpha}_0$ [fm]	$\hat{\alpha}_1$ [fm]	E_B [MeV]
V_5	5	-24.51	65.717	24.46	-14.22	-2.225
V_{10}	10	-23.71	129.017	24.43	-14.18	-2.225
V_{20}	20	-23.49	262.321	24.40	-14.17	-2.225

calculated using the coordinate-space method described in Appendix C. The low-energy scattering parameters $\hat{\alpha}_0, \hat{\alpha}_1$, introduced in Appendix A, were calculated numerically with the same method.

These potentials have a simple representation also in momentum-space

$$V\left(k,k'\right) = \frac{\beta}{\pi}\left(\frac{V_A}{\left(k-k'\right)^2+\beta^2} + \frac{nV_B}{\left(k-k'\right)^2+\left(n\beta\right)^2}\right) \tag{52}$$

and it has been checked that the numerical calculations done in momentum space are consistent with the results obtained with the coordinate-space method.

The bound-state energies of the three-body system are found by the condition that the generalized eigenvalue in Eq. (48) has to be equal to one. We investigated the effect of the correction terms for the three potentials V_5, V_{10}, and V_{20}. Note that the coupling constant of the force-mediating boson is implicitly defined by the two-body potential, since the boson-exchange potential is given by the exponential

$$\frac{f^2}{\beta}e^{-\beta|x|}. \tag{53}$$

This is the analogue of the Yukawa potential in one dimension. Hence the correction terms discussed in section 3 have to be evaluated with the condition $f^2 = \beta V_A$.

In Fig. 4 we show the convergence behaviour of the three-body binding energy in respect to the rank of the separable expansion for the three potentials. The left graph shows the convergence of the calculation without any correction terms

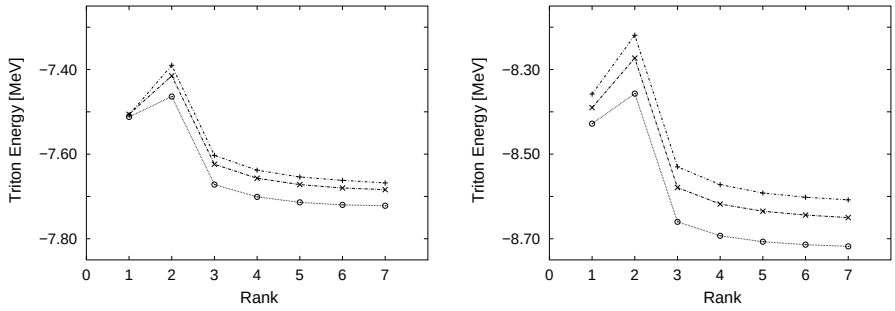

Figure 4. Convergence behavior of the binding energy for the three potentials in respect to the rank of the UPE. The left graph shows the calculation with no correction terms and the right one with both correction terms (diagonal and off-diagonal) included. The ∘ denote the results for potential V_5, the × for potential V_{10} and the + for potential V_{20}.

and the right one with both corrections (diagonal and off-diagonal). The two effective parameters c_1 and c_2 have been set to -15 and 1, respectively. It is clearly seen that both calculations show a convergence in respect to the rank of the UPE. In Table 2 we show the numerical results for rank 7 calculations

Table 2. 'Triton' energies in MeV for the three potentials, including different 3NF corrections. The results are given for a rank 7 UPE and with an effective parameter $c_2 = 1$

	2NF	2NF+OPE3	2NF+TPE3	2NF+OPE3+TPE3
V_5	-7.722	-7.708	-8.733	-8.718
V_{10}	-7.684	-7.662	-8.670	-8.650
V_{20}	-7.668	-7.642	-8.631	-8.608

with different combinations of correction terms. It is worth noting that, once the local two-body potential has been constructed to mimic the properties of the three-dimensional 2N system (2N binding energy and low energy parameters), the three-body binding energy turns out remarkably close to the values expected for the 3N system, in spite of the fact that we have considered a rather different system, namely three spinless bosons defined in one dimension.

It has also to be observed that the off-diagonal pionic contributions, originated by the TPE3 diagram of Fig. 1 can indeed be modelled to correct a hypothetical under-binding of the three-body system, since these terms have the potential to provide an additional contribution to the binding energy which can be sized around 0.9 MeV. This also presents interesting analogies with the 3-D case of realistic 3N system. We stress, however, that details can change, also significantly, depending on the particular model considered for the off-shell extrapolation of the πN amplitude.

The diagonal correction terms related to the OPE3 diagram (Fig. 3) produce

changes in the three-body binding energies which are significantly smaller than the off-diagonal ones. This also presents interesting analogies with the realistic 3N case [28], where it has been already found that the triton binding energy is not strongly affected by the diagonal correction terms. Within this 1-D model one could conclude that they could be neglected in first instance, if the effective parameter c_2 is set to one.

Of course, this should not lead to the assumption that the OPE3 terms can also be ignored in calculations of other observables, as it happens for the case of the vector analyzing powers, for realistic nucleon-deuteron scattering at low energy. It was shown in refs. [28, 29] that the effective parameter c_2 can be fitted to the peak of the A_y-data. The value of the parameter in these fits depends sensitively on the particular NN-potential used in the calculations, but in every case the resulting curves reproduce the existing data base quite well. Finally, it is worth mentioning that the two correction terms produce additive effects to the three-body binding.

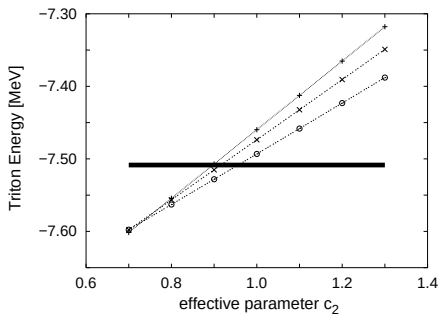

Figure 5. Dependence of the binding energy on the parameter c_2 in a rank 1 calculation for all three potentials including the diagonal correction terms. The ∘ denote the results for potential V_5, the × for potential V_{10} and the + for potential V_{20}. The thick line denotes the triton energy without any correction terms for all three potentials.

In Fig. 5 we show how varying the parameter c_2 affects the binding energy in the one-dimensional three-body model. The range of variation for c_2 shown in the figure is consistent with the values for c_2 found in refs. [28, 29]. As mentioned earlier, one possible reason for using c_2 as an adjustable parameter is the fact that the 2N t-matrix entering in the OPE3 diagram has to be calculated off the energy shell, in a region which is difficult to constrain by experimental data. In addition, the figure reveals how the variations with c_2 are dependent also on the selection of the two-body potential. At a parameter value of 0.7 the diagonal correction terms introduce an effect that is approximately 10% of the effect introduced by the off-diagonal correction terms. At a value of 1.3 the effect is in the opposite direction and the magnitude of the effect is strongly dependent on the particular potential, as seen by the different slopes. We have chosen to show the rank 1 calculation for different potentials, because the binding energies without correction terms are practically equal for all three potentials in this case. However, the same behavior can also be observed in the higher-rank calculations. We conclude that, a priori, one should not neglect the diagonal terms in this model calculation.

6 Summary and Conclusion

The scope of this study was originally the development of a strongly simplified toy model in which to test a three-nucleon theory with residual pionic corrections, namely with contributions that could not be described via conventional two-nucleon potentials. The general theoretical framework adopted as starting point has been the coupled equations of ref. [25] for the πNNN-NNN system, further reduced in ref. [26] to an approximate but more practical three-body dynamical equation with irreducible pionic corrections.

For this scope we formulated the quantum mechanical three-body problem in one-dimension, on the $(-\infty, +\infty)$ line, and considered the addition of two different 3NF-type diagrams generated by the residual pion dynamics. In the specialized literature, attention has been focused – also recently – to these types of diagrams in realistic 3N studies for both bound and scattering regimes.

In this work, we concentrated our numerical study on the binding energies of the three-body system. We described the gross features of the 3-body bindings, observing also interesting analogies with the more realistic 3N-bound states, despite the rather severe simplifications introduced by the one-dimensional model.

In particular, using simple 1-D potentials that could reproduce the deuteron energy, we obtained a 3-body binding of about 7.5 MeV. Addition of residual pionic diagrams of the "TPE3" type (Fig. 2) carries an additional binding of about 0.9 MeV. However, significant model dependence on the structure of the "πN" amplitude (related to these diagrams) can and have to be expected. The addition of the second type of diagrams, denoted "OPE3" (see Fig. 3), produces an additional effect on the binding which is either negligible or moderate, depending on the specifics of the selected two-body potential, and on the value of an effective parameter that governs such diagrams. It must be observed that one cannot conclude that the OPE3 terms are less important, since they could quite significantly affect other three-body observables. This indeed turned out to be the case for the nucleon-deuteron A_y observable in realistic studies [28, 29].

However, we realized also that the 1-D approach we developed for the scopes discussed above went somehow beyond the initial intentions of the authors. In fact it turned out, to the best of our knowledge, that the three-body quantum scattering theory using the Faddeev-AGS-Lovelace formulation in terms of coupled integral equations has never been discussed before for one-dimensional systems, while the general formulation for such systems could attract interest in various fields dealing with one-dimensional systems. For this reason, we have devoted Sect. 2 to the general discussion of the quantum-mechanical 3-body scattering problem in one dimension. Both cases involving distinguishable or identical particles have been formulated in terms of the integral-equation approach.

As possible applications and future extensions of the 1-D model considered herein, one could consider also other cases of three-body models where there is the need of an explicit coupling to the meson degree of freedom. This is the case, for example, of the constituent quark model based on Goldstone-boson exchanges [49], which provided a rather realistic description of the excitation spectra of all light and strange baryons [50]. One might think to improve the description of the excitation spectra by including explicit mesonic degrees of

freedom into the resonance states, and in this framework to study the π and η decay modes of N and Δ resonances. Another possible application is in η-3N scattering [51] and associated reactions [52]. These processes are dynamically coupled with the absorption channel, and with the π-channel itself, and therefore the dynamics is highly complicated. In both these examples, it would be rather useful to develop similar 1-D models as theoretical laboratory where to test methods, approximations, and dynamical assumptions in a simplified framework.

Acknowledgement. We acknowledge support from the Italian MURST-PRIN Project "Fisica Teorica del Nucleo e dei Sistemi a Più Corpi". T.M. acknowledges support from the University of Manitoba. J.P.S. acknowledges support from the Natural Science and Engineering Research Council of Canada. The authors also would like to thank the Institutions of INFN (Padova), University of Manitoba, and Università di Padova for hospitality during reciprocal visits.

Appendix A: Partial Waves and Low Energy Behaviour in One-Dimensional Scattering

Here we review some general results obtained in 1-D scattering theory. We consider a particle of mass m with no internal degrees of freedom subject to a potential $V(x)$ in one dimension. The potential is assumed to be real and approaching zero sufficiently fast for $x \to \pm\infty$. Furthermore, we restrict our investigation to symmetric potentials $V(x) = V(-x)$. The Schrödinger equation for this problem is

$$-\frac{d^2\Psi_k(x)}{dx^2} + U(x)\,\Psi_k(x) = k^2\Psi_k(x)\ , \tag{A.1}$$

where $k = (2mE)^{\frac{1}{2}}/\hbar$ is the wave number, E is the energy of the particle and $U(x) = \left(2m/\hbar^2\right)V(x)$. In this section we examine the transmission-reflection problem for positive energies. This problem has two independent solutions with incident waves from the left and right respectively. The asymptotic form for the wave function incident from the left is given by

$$\Psi_k^L(x) \to \begin{cases} e^{\mathrm{i}kx} + R_L(E)\,e^{-\mathrm{i}kx}, & \text{for } x \to -\infty \\ T_L(E)\,e^{\mathrm{i}kx}, & \text{for } x \to +\infty\,. \end{cases} \tag{A.2}$$

The transmission and reflection coefficients T_L, R_L lead to the transmission and reflection probabilities, which have to satisfy

$$|T_L(E)|^2 + |R_L(E)|^2 = 1 \tag{A.3}$$

due to conservation of probability. The asymptotic form for the wave function incident from the right is defined similarly replacing x with $-x$.
The S-matrix is given according to the definition [35, 37]

$$S(E) = \begin{pmatrix} T_L(E) & R_R(E) \\ R_L(E) & T_R(E) \end{pmatrix}\ , \tag{A.4}$$

which reduces to the identity matrix when the potential goes to zero. In general, the matrix elements are complex and hence the matrix is defined by eight real parameters. Unitarity of the S-matrix leads to four constraints on the matrix elements and for real and symmetric potentials two more constraints are observed. This leads to the identity of the transmission and reflection coefficients for the incident waves from the left and right

$$T(E) = T_L(E) = T_R(E) \tag{A.5}$$

$$R(E) = R_L(E) = R_R(E)\ , \tag{A.6}$$

which represent the only two independent parameters of the S-matrix

$$S(E) = \begin{pmatrix} T(E) & R(E) \\ R(E) & T(E) \end{pmatrix}\ . \tag{A.7}$$

In the one-dimensional scattering problem there are two partial waves, one with even parity and one with odd parity. The $\mathcal{S}$-matrix in respect to these partial waves for real and symmetric potentials is found by a diagonalization procedure

$$\mathcal{S}(E) = \begin{pmatrix} T(E) + R(E) & 0 \\ 0 & T(E) - R(E) \end{pmatrix}. \tag{A.8}$$

Furthermore, due to the unitarity of the S-matrix, it can also be given in the partial wave representation

$$\mathcal{S}(E) = \begin{pmatrix} e^{2i\delta_0(E)} & 0 \\ 0 & e^{2i\delta_1(E)} \end{pmatrix}, \tag{A.9}$$

where $\delta_{0,1}(E)$ are real and define the phase shifts of the scattering process [53, 54]. In Fig. A.1 we show the odd and even phase shifts calculated with the procedure described in Appendix C. They show the behaviour expected from the one-dimensional Levinson theorem [37, 38], namely

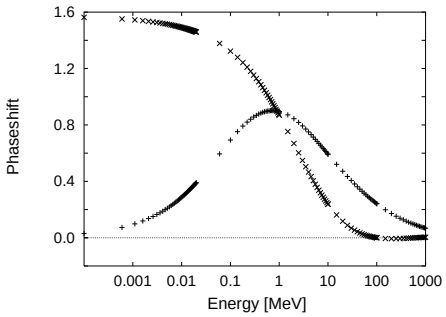

Figure A.1. Phase shifts for the odd and even wave function with potential V_{20}, + denotes the odd phase shift and × the even phase shift.

the odd phase goes to zero at threshold and the even to $\frac{\pi}{2}$, because of the even bound state. For completeness, we note that the transmission and reflection coefficients can also be expressed in respect to the phase shifts in the following way

$$T(E) = \frac{1}{2}\left(e^{2i\delta_0(E)} + e^{2i\delta_1(E)}\right) = \cos\left(\delta_0(E) - \delta_1(E)\right) e^{i(\delta_0(E)+\delta_1(E))} \tag{A.10}$$

$$R(E) = \frac{1}{2}\left(e^{2i\delta_0(E)} - e^{2i\delta_1(E)}\right) = \sin\left(\delta_0(E) - \delta_1(E)\right) e^{i\left(\delta_0(E)+\delta_1(E)+\frac{\pi}{2}\right)}. \tag{A.11}$$

Finally, according to Galindo and Pascual [6], for potentials that go to zero sufficiently fast, when x goes to plus or minus infinity, the following generic behavior is observed

$$T(E) \approx \alpha_0\sqrt{\frac{2mE}{\hbar^2}}, \qquad \sqrt{\frac{2mE}{\hbar^2}} \to 0 \tag{A.12}$$

$$R(E) \approx -1 + \alpha_1\sqrt{\frac{2mE}{\hbar^2}}, \qquad \sqrt{\frac{2mE}{\hbar^2}} \to 0, \tag{A.13}$$

where α_0, α_1 are generally complex constants not equal to zero. Therefore, the S-matrix in the low-energy limit tends to a total reflection. It should be noted that, for the specific type of potentials we use, it turns out the constants α_0, α_1 are purely imaginary numbers.

The transmission and reflection coefficients can be calculated by resorting to the Green's function formalism [31, 36]. The Schrödinger Eq. (A.1) can be written in integral form, which leads to the Lippmann-Schwinger equation

$$\Psi_k(x) = \Phi_k(x) + \int_{-\infty}^{+\infty} G_0(x, x')\, U(x')\, \Psi_k(x')\, dx', \tag{A.14}$$

where $\Phi_k(x)$ is a solution of the free Schrödinger equation and the Green's function $G_0(x,x')$ is defined incorporating the boundary conditions of the equivalent Schrödinger problem. For 1-D systems the Green's function with outgoing boundary conditions has the following form

$$G_0(x,x') = -\frac{\mathrm{i}}{2k} e^{ik|x-x'|}. \tag{A.15}$$

The general solution of the free Schrödinger Eq. (A.1) is given by

$$\Phi_k(x) = Ae^{\mathrm{i}kx} + Be^{-\mathrm{i}kx}, \tag{A.16}$$

where the coefficients A and B are arbitrary. Inserting these expressions in the Lippmann-Schwinger equation leads directly to the following equation

$$\begin{aligned}\Psi_k(x) &= Ae^{\mathrm{i}kx} + Be^{-\mathrm{i}kx} \\ &\quad - \frac{\mathrm{i}m}{\hbar^2 k}\left[\int_{-\infty}^{x} e^{\mathrm{i}k(x-x')} V(x')\Psi_k(x')\,dx' + \int_{x}^{+\infty} e^{\mathrm{i}k(x'-x)} V(x')\Psi_k(x')\,dx'\right]\end{aligned} \tag{A.17}$$

and A, B can now be determined according to the various boundary conditions. One choice is $A = 1, B = 0$ and corresponds to the following equation

$$\Psi_k^L(x) = e^{\mathrm{i}kx} - \frac{\mathrm{i}m}{\hbar^2 k}\left(\int_{-\infty}^{+\infty} e^{\mathrm{i}kx'} V(x')\Psi_k^L(x')\,dx'\right) e^{-\mathrm{i}kx} \qquad x \to -\infty \tag{A.18}$$

$$\Psi_k^L(x) = \left[1 - \frac{\mathrm{i}m}{\hbar^2 k}\left(\int_{-\infty}^{+\infty} e^{-\mathrm{i}kx'} V(x')\Psi_k^L(x')\,dx'\right)\right] e^{\mathrm{i}kx} \qquad x \to +\infty, \tag{A.19}$$

which is equivalent to the previously defined solution in Eq. (A.2). The transmission and reflection coefficients for scattering with an incoming wave from the left are then given by the expressions

$$T_L(E) = 1 + \frac{\mathrm{i}}{2k} f_+^{kL} \tag{A.20}$$

$$R_L(E) = \frac{\mathrm{i}}{2k} f_-^{kL}, \tag{A.21}$$

where

$$f_\pm^{kL} = -\frac{2m}{\hbar^2}\int_{-\infty}^{+\infty} e^{\mp \mathrm{i}x'k} V(x')\Psi_k^L(x')\,dx' \tag{A.22}$$

is the scattering amplitude for an incoming wave from the left. In a similar way it is possible to describe the scattering system with an incoming wave from the right by choosing the coefficients $A = 0, B = 1$. However, we already argued that for the type of potentials we use in this paper the left- and right- coefficients are equal. Therefore, we drop the indices L, R in the remainder of this section and denote the scattering amplitude in both directions by $f_\pm^k$. Observing that in the one-dimensional system, for a given energy E, there exist exactly two possible momenta

$$k_\pm = \pm\frac{\sqrt{2mE}}{\hbar} \tag{A.23}$$

we define the on-shell t-matrices by the expression

$$\begin{aligned} t(k_\pm, k; E) &= \langle k_\pm | t(E) | \Phi_k \rangle = \langle \Phi_{\pm k} | V | \Psi_k \rangle \\ &= \int_{-\infty}^{+\infty} e^{\pm \mathrm{i}kx'} V(x')\Psi_k(x')\,dx' = -\frac{\hbar^2}{2m} f_\pm^k. \end{aligned} \tag{A.24}$$

For the off-the-energy-shell situation the t-matrix is introduced according to

$$t(E)|\Phi_q\rangle = V|\Psi_q\rangle \tag{A.25}$$

and it can be calculated by the Lippmann-Schwinger equation

$$t(E) = V + VG_0 t(E) \tag{A.26}$$

which reads in momentum-space

$$t\left(q,q';E\right)=V\left(q,q'\right)+\int_{-\infty}^{+\infty}V\left(q,q''\right)G_0\left(q'',E\right)t\left(q'',q';E\right)dq'' \tag{A.27}$$

where

$$G_0\left(q,E\right)=\left(E-\frac{\hbar^2q^2}{2M}\right)^{-1} \tag{A.28}$$

Finally, combining Eqs. (A.4,A.20,A.21,A.24) it is possible to express the S-matrix in respect to the on-shell t-matrix

$$S\left(E\right)=\begin{pmatrix}1&0\\0&1\end{pmatrix}-\frac{im}{\hbar^2k}\begin{pmatrix}t\left(k,k;E\right)&t\left(k,-k;E\right)\\t\left(-k,k;E\right)&t\left(-k,-k;E\right)\end{pmatrix}. \tag{A.29}$$

A diagonalization procedure lets us express this result in terms of two "partial wave" t-matrices

$$\mathcal{S}\left(E\right)=\begin{pmatrix}1&0\\0&1\end{pmatrix}-\frac{im}{\hbar^2k}\begin{pmatrix}t_0\left(E\right)&0\\0&t_1\left(E\right)\end{pmatrix}, \tag{A.30}$$

where

$$\begin{aligned}t_0\left(E\right)&=t\left(k,k;E\right)+t\left(k,-k;E\right)\\t_1\left(E\right)&=t\left(k,k;E\right)-t\left(k,-k;E\right)\end{aligned} \tag{A.31}$$

The low energy behavior of the t-matrix can be defined by a direct comparison to the low energy behavior of the on-shell S-matrix, which yields

$$t_0\left(E\right)\approx-\frac{\hbar^2}{im}\sqrt{\frac{2mE}{\hbar^2}}\left[\left(\alpha_0+\alpha_1\right)\sqrt{\frac{2mE}{\hbar^2}}-2\right] \tag{A.32}$$

$$t_1\left(E\right)\approx-\frac{\hbar^2}{im}\sqrt{\frac{2mE}{\hbar^2}}\left(\alpha_0-\alpha_1\right)\sqrt{\frac{2mE}{\hbar^2}}, \tag{A.33}$$

where $0,1$ denote the even and odd t-matrix respectively. In Fig. A.2 we show the low energy behaviour of the transmission and reflection coefficients explicitly. The figures were calculated using the procedure outlined in Appendix C. Clearly, the imaginary parts of the reflection and

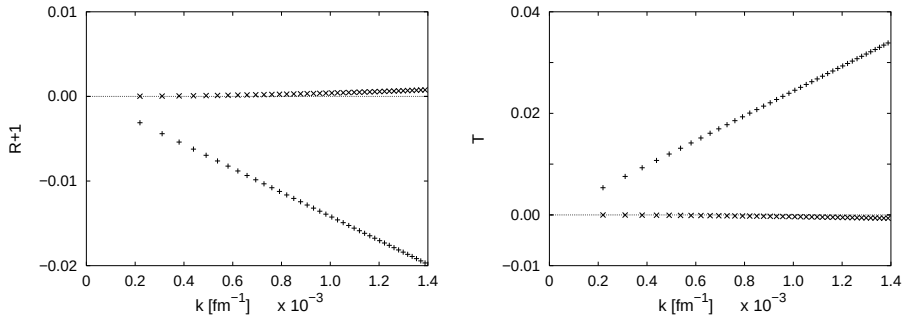

Figure A.2. Real and imaginary parts of the coefficients $R+1$ and T. The $+$ denote the imaginary parts of the coefficients, the $\times$ denote the real parts of the coefficients.

transmission coefficients show the linear behaviour, while the real parts are equal to zero. In the TPE3 a subtracted πN t-matrix enters and we approximate it by the definition

$$t_F\left(q,q'\right)=-\frac{\hbar^2}{m}\left[\frac{\left(\hat{\alpha}_0+\hat{\alpha}_1\right)\left|q\right|\left|q'\right|+\left(\hat{\alpha}_0-\hat{\alpha}_1\right)qq'}{2}\right]. \tag{A.34}$$

Here, the parameters $\hat{\alpha}_0,\hat{\alpha}_1$ denote the imaginary parts of α_0,α_1, which are given by the Eqs. (A.12,A.13). Furthermore, to get this result from Eqs. (A.32,A.33), it must be observed

that both odd and even terms must be added coherently, since the meson and the nucleon are distinguishable. Finally, we have neglected the additional contribution due to the presence of the term -1 in Eq. (A.13). This contribution originates because in the low-energy limit the 1-D scattering event becomes a purely reflective process ($T \to 0$, $R \to -1$). It is eliminated from Eq. (38) because in the πN t-matrix there are contributions that need to be subtracted, i.e. the forward propagating nucleon diagram and its crossed counterpart. In the three-dimensional case, the subtraction of such diagrams is discussed for example in ref. [24]. Finally, a phenomenological constant c_1 has to be introduced to account for the different magnitudes of the low energy πN and NN t-matrices. For insertion into the off-diagonal correction terms the expression is rewritten in the appropriate units multiplying it by the constant $(2m)/\hbar^2$.

Appendix B: The unitary pole expansion

In this appendix we describe the Unitary Pole Expansion (UPE), which is the input for our three-body bound state problem. The UPE is closely related to the Weinberg series [55] and is described by Harms [56]. We derive the UPE in a slightly different, but equivalent, way as discussed by Pisent et al. [48]. The homogeneous form of the Lippmann-Schwinger Equation (A.26) can be given by the generalized eigenvalue equation

$$VG_0(E)V|\phi_n(E)\rangle = \eta_n(E)V|\phi_n(E)\rangle \ . \tag{B.1}$$

The form factors of the separable expansion are defined by

$$|\chi_n(E)\rangle = V|\phi_n(E)\rangle \ . \tag{B.2}$$

In our case we have only one bound state and we choose to use the expansion at the bound state energy $E = -B$. In this way we recover the Unitary Pole Expansion (UPE). Furthermore, it is easily seen that the first eigenvalue $\eta_1(E)$ is equal to one in this case. Therefore, the bound state $|\phi_B\rangle$ and the first form factor in the expansion satisfy the relation

$$|\chi_1\rangle = V|\phi_B\rangle \ . \tag{B.3}$$

The bound state calculated with this definition was compared to the one calculated with the Fox-Goodwin method and it was seen that they indeed do agree with each other. It is also known [48] that the eigenvectors of Eq. (B.1) have the following orthogonality relation

$$\langle\phi_n|V|\phi_m\rangle = -\eta_n\delta_{nm} \ , \tag{B.4}$$

where the $|\phi_m\rangle$ are the solutions of Eq. (B.1) at the binding energy $E = -B$. This orthogonality relation also specifies the normalization of the eigenfunctions, which is slightly different from that introduced in Section 2. The two-body potential V is given in respect to the following separable expansion

$$V = -\sum_i \frac{|\chi_i\rangle\langle\chi_i|}{\eta_i} \tag{B.5}$$

and the separable T matrix is given by

$$T = \sum_{i,j} |\chi_i\rangle \Delta_{ij} \langle\chi_j| \ , \tag{B.6}$$

where the matrix elements of Δ are defined by the expression

$$\left[\Delta^{-1}\right]_{ij} = -\eta_i\delta_{ij} - \langle\chi_i|G_0|\chi_j\rangle \ . \tag{B.7}$$

In the case that only one term in this expansion is retained the expansion reduces to the Unitary Pole Approximation (UPA) discussed by Lovelace [43] and Fuda [57]

$$T_{UPA} = |\chi_1\rangle \Delta_{11} \langle\chi_1| \tag{B.8}$$

with

$$\Delta_{11} = -\left[1 + \langle\chi_1|G_0|\chi_1\rangle\right]^{-1} \ . \tag{B.9}$$

It is easily seen that both the UPE and UPA have the right pole structure, namely the separable T matrix has a pole at the bound state energy.

Appendix C: Numerical Studies of the Two-Body Problem in Coordinate Space

We note that our one-dimensional system is defined on the whole line and not the half line like the radial Schrödinger equation of a three-dimensional problem. In this Appendix we show how the system can be solved numerically for any finite-range symmetric potential.
The problem is defined by the time-independent Schrödinger equation

$$H\psi(x) = E\psi(x) \,, \tag{C.1}$$

which can be written as

$$u''(x) + w(x)\, u(x) = 0 \,, \tag{C.2}$$

where

$$w(x) = \frac{2m}{\hbar^2}\left(E - V(x)\right) \,. \tag{C.3}$$

The Fox-Goodwin method [58] replaces the differential equation by a finite expression

$$u(x+h) = \frac{2u(x) - u(x-h) - \left(\frac{h^2}{12}\right)\left(10w(x)\, u(x) + w(x-h)\, u(x-h)\right)}{1 + \left(\frac{h^2}{12}\right) w(x+h)} \,, \tag{C.4}$$

which is exact to the order of h^4. If one knows the values of the function u at the positions 0 and h, then it is possible to calculate the value of the function at the point $2h$. Repeating this procedure with the function at h and $2h$ will give its value at $3h$ and so on. With this procedure the function is defined on a grid with discretization interval h. The first two values chosen in this procedure, namely $u(0)$ and $u(h)$ depend on the boundary conditions of the system. This procedure works well for the radial equation, because one has a definite starting point at zero.

The generalization to the full line is simplified if one takes advantage of the symmetric nature of the potential. The symmetry implies that the eigenstates can be classified into symmetric (even) or anti-symmetric (odd) states. Therefore, it is possible to restrict the calculation to the positive part of the real line by imposing the appropriate boundary conditions at the origin for both odd and even states.

Odd states have to go through zero at the origin. Consequently, we define the boundary conditions at the origin in the following way

$$u_1(0) = 0 \qquad u_1(h) = 1 \,. \tag{C.5}$$

Even states have to go through an extremum at zero, but without crossing the origin. Consequently, we define the symmetric boundary conditions as follows ($h \to 0$)

$$u_0(0) = 1 \qquad u_0(h) = 1 \,. \tag{C.6}$$

C.1 The Bound State Problem on the Real Line

Bound-state solutions, in both odd and even cases, have to be normalizable. In the positive direction, negative-energy solutions follow the asymptotic behaviour

$$u(x) = ae^{-\kappa x} + be^{\kappa x} \,, \tag{C.7}$$

with $\kappa = \sqrt{2m\,|E|}/\hbar$ being the wave number for $E < 0$.

The normalization condition determines the bound-state by selection of the energies corresponding to a zero of the b coefficient, namely a vanishing wavefunction for $x \to +\infty$. Numerically, the bound states and energies are found by starting the Fox-Goodwin algorithm at $x = 0$ with either the odd and even Conditions (C.6,C.5), and then evaluating the wavefunction for very large x values. Generally, the function assumes very large values, due to the increasing exponent in Eq. (C.7), except for energy values corresponding to bound states, where the wavefunction drops to zero at large distances and becomes normalizable.

C.2 The Scattering Problem on the Real Line

The 1-D scattering problem is solved separately for antisymmetric and symmetric states by starting at the origin with either Condition (C.6) or (C.5), and propagating the solution in the asymptotic region $x \to +\infty$ with the Fox-Goodwin method. In the odd case we know that the solution in the asymptotic region has to be of the form

$$\bar{u}_1(x) = a_1 \sin(kx + \delta_1) \tag{C.8}$$

with $k = \sqrt{2mE}/\hbar$ being the wave number and the bar denoting the asymptotic solution.

Equating the last two points of the numerical solution with this general expression gives the following two equations

$$\begin{aligned} u_1(B) &= a_1 [\cos(\delta_1)\sin(kB) + \sin(\delta_1)\cos(kB)] \\ u_1(B-h) &= a_1 [\cos(\delta_1)\sin(k(B-h)) + \sin(\delta_1)\cos(k(B-h))] , \end{aligned} \tag{C.9}$$

where B and $B-h$ are the largest and second largest x-value at which the wavefunction is calculated numerically. Solution of this system leads to the following expression defining the phase shift

$$\tan(\delta_1) = \frac{\sin[k(B-h)]\,u_1(B) - \sin[kB]\,u_1(B-h)}{-\cos[k(B-h)]\,u_1(B) + \cos[kB]\,u_1(B-h)} . \tag{C.10}$$

Substituting the phase shift back into (C.9) gives also the odd amplitude a_1.

The even phase shift can be similarly determined by the asymptotic behavior

$$\bar{u}_0(x) = a_0 \cos(kx + \delta_0) , \tag{C.11}$$

which yields

$$\tan(\delta_0) = \frac{\cos[kB]\,u_0(B-h) - \cos[k(B-h)]\,u_0(B)}{\sin[kB]\,u_0(B-h) - \sin[k(B-h)]\,u_0(B)} . \tag{C.12}$$

As for the antisymmetric case, also the symmetric amplitude a_0 can be determined in the same way.

Generally, the asymptotic behavior of the one dimensional scattering system for incoming waves from the left ($x \to -\infty$), is described by

$$\bar{u}(x \to -\infty) = e^{ikx} + R \cdot e^{-ikx} \tag{C.13}$$

$$\bar{u}(x \to +\infty) = T \cdot e^{ikx} , \tag{C.14}$$

where R and T denote the reflection and transmission coefficients. We define the scattering wavefunction $u(x)$ with the proper asymptotic behaviour by a (suitably chosen) linear combination of odd and even solutions, namely

$$u(x) = \frac{e^{i\delta_0}}{a_0} u_0(x) + i\frac{e^{i\delta_1}}{a_1} u_1(x) . \tag{C.15}$$

Comparing the asymptotic behaviour for both antisymmetric and symmetric Solutions C.8 C.11 with the Form C.13 C.14 one derives the two scattering coefficients

$$T(E) = \frac{1}{2}\left(e^{2i\delta_0(E)} + e^{2i\delta_1(E)}\right) \tag{C.16}$$

$$R(E) = \frac{1}{2}\left(e^{2i\delta_0(E)} - e^{2i\delta_1(E)}\right) , \tag{C.17}$$

according to the expressions already mentioned in Appendix A.

References

1. Ha, Z. N. C.: Quantum many-body systems in one dimension (Adv. in Stat. Mech., Vol. **12**). Singapore: World Scientific 1996
2. Hauge, E. H., Stovneg, J. A.: Rev. Mod. Phys. **61**, 917 (1989)
3. Itoh, T.: Phys. Rev. B **52**, 1508 (1995)
4. Simon, B.: J. Math. Phys. **41**, 3523 (2000)
5. Lipkin, H. J.: Quantum mechanics, new approaches to selected topics. Amsterdam :North-Holland Publishing Company 1973
6. Galindo, A., Pascual, P.: Quantum mechanics I. Berlin: Springer Verlag 1990
7. Barlette V. E., Leite M. M., Adhikari S. K.: Eur. J. Phys. **21**, 435 (2000)
8. Alt, E. O., Grassberger, P., Sandhas, W.: Nucl. Phys. **B2**, 167 (1967)
9. Grassberger, P., Sandhas, W.: Nucl. Phys. **B2**, 181 (1967)
10. Faddeev, L. D.: Zh. Eksp. Teor. Fiz. **39**, 1459 (1960); [Sov Phys. JETP **12**, 1014 (1961)]
11. Yakubovski, O. A.: Sov. J. Nucl. Phys. **5**, 937 (1967)
12. Hegerfeldt, G. C., Köhler, T.: In: Few-body problems in physics '98: Proceedings of the 16th European conference on few-body problems in physics, Autrans, France, June 1-6, 1998, (Desplanques, B., et al., eds.) Few-Body Syst. Suppl. 10, p. 263. Berlin: Springer Verlag 1999
13. Lacombe, L., et al.: Rev. C **21**, 61 (1980)
14. Machleidt, R., Holinde, K., Elster, Ch.: Phys. Rep. **149**, 1 (1987)
15. Stoks, V. G. J., et al.: Phys. Rev. C **49**, 2950 (1994)
16. Wiringa, R. B., Stoks, V. G. J., Schiavilla, R.: Phys. Rev. C **51**, 38 (1995)
17. Machleidt, R.: Phys. Rev. C **63**, 024001 (2001)
18. Glöckle, W., et al.: Phys. Rep. **274**, 107 (1996)
19. Knutson L. D.: In: Few-body problems in physics: Proceedings of the XVth international [IUPAP] conference on few-body problems in physics, Groningen, The Netherlands, 22-26 July 1997, (Bacelar J. C. S., et al., eds.) Nucl. Phys. **A631**, p. 9c. Amsterdam: Elsevier Science B. V. 1998
20. Fujita, J., Miyazawa, M.: Prog. Theor. Phys. **17**, 360 (1957)
21. Coon, S. A., et al.: Nucl. Phys. **A317**, 242 (1979)
22. Robilotta, M. R., Coelho, H. T.: Nucl. Phys. **A460**, 645 (1986)
23. Ordonez, C., van Kolck, U.: Phys. Lett. **B291**, 459 (1992)
24. van Kolck, U.: Phys. Rev. C **49**, 2932 (1994)
25. Canton, L.: Phys. Rev. C **58**, 3121 (1998)
26. Canton, L., Melde, T., Svenne, J. P.: Phys. Rev. C **63**, 034004 (2001)
27. Canton, L., Schadow, W.: Phys. Rev. C **62**, 044005 (2000)
28. Canton, L., Schadow, W.: Phys. Rev. C **64**, 031001(R) (2001)
29. Canton, L., Schadow, W., Haidenbauer, J.: nucl-th/0111045 (2001)
30. Canton, L., et al.: Theoretical nuclear physics in Italy, Proceedings of the 8th Conference on Problems in Theoretical Nuclear Physics, Cortona, Italy, October 18-20 (Pisent, G., et al., eds.), p. 249. Singapore: World Scientific 2001
31. Melde, T.: Ph.D. Thesis. Univ. of Manitoba 2001 (unpublished)
32. Miyazawa, T.: J. Phys. A **33**, 191 (2000)
33. Rybkin, A.: Proc. Am. Math. Soc. **130**, 59 (2001)
34. Aktosun, T., Klaus, M., and van der Mee, C.: J. Math. Phys. **42**, 4627 (2001)

35. Nogami, Y., Ross, C. K.: Am. J. Phys. **64**, 923 (1996)
36. Barlette, V., Leite, M., Adhikari, S. K.: Am. J. Phys. **69**, 1010 (2001)
37. Sassoli de Bianchi, M.: J. Math. Phys. **35**, 2719 (1994)
38. Bolle, D., Gesztesy, F., Klaus, M.: J. Math. Analysis and Appl. **122**, 496 (1987)
39. Bolle, D., Gesztesy, F., Wilk, F. J.: J. Operator Theory **13**, 3 (1985)
40. McGuire, J. B.: J. Math. Phys. **5**, 66 (1964)
41. Taylor, J. R.: Scattering theory. New York: John Wiley & Sons, Inc. 1972
42. Glöckle, W.: The quantum mechnical few-body problem. Berlin: Springer Verlag 1983
43. Lovelace, C.: Phys. Rev. **135**, B1225 (1964)
44. Schmid, E. W., Ziegelmann, H.: The quantum mechanical three-body problem. Braunschweig: Friedr. Vieweg und Sohn Verlagsgesellschaft mbH 1974
45. Ericson, T., Weise, W.: Pions and Nuclei. Oxford: Oxford Science Publications 1998
46. Adhikari, S. K., Kowalski, K. L.: Dynamical collision theory and its applications San Diego: Academic Press, Inc. 1991
47. Sitenko, A. G.: Scattering theory. Berlin: Springer Verlag 1991; [Tr. from the 1975 Russian edition by Kocheroga, O. D.]
48. Pisent, G., et al.: Phys. Rev. C **48**, 64 (1993)
49. Glozman, L. Ya., Riska, D. O.: Phys. Rep. **268**, 263 (1996)
50. Glozman, L. Ya., Plessas, W., Varga, K., Wagenbrunn, R. F.: Phys. Rev. D **58**, 094030 (1998)
51. Fix, A., Arenhövel, H.: arXiv:nucl-th/0202080v1, preprint MKPH-T-02-01
52. Shevchenko, N. V., et al.: arXiv:nucl-th/0108031
53. Eberly, J. H.: Am. J. Phys. **33**, 771 (1965)
54. Formanek, J.: Am. J. Phys. **44**, 778 (1976)
55. Weinberg, S.: Phys. Rev. **131**, 440 (1963)
56. Harms, E.: Phys. Rev. C **1**, 1667 (1970)
57. Fuda, M. G.: Nucl. Phys. **A116**, 83 (1968)
58. Schmid, E. W., Spitz, G., Loesch, W.: Theoretical physics on the personal computer. Berlin: Springer Verlag 1988